UCLA
UCLA Electronic Theses and Dissertations

Title
Photothermal Nanoblade Delivery of Wild-type Mitochondria into mtDNA Depleted Osteosarcoma Cells

Permalink
https://escholarship.org/uc/item/6861x8gz

Author
Zheng, Xin

Publication Date
2012

Peer reviewed|Thesis/dissertation

eScholarship.org Powered by the California Digital Library
University of California

UNIVERSITY OF CALIFORNIA

Los Angeles

Photothermal Nanoblade Delivery of Wild-type Mitochondria into mtDNA Depleted Osteosarcoma Cells

A thesis submitted in partial satisfaction

of the requirements for the degree Master of Science

in Biomedical Engineering

by

Xin Zheng

2012

© Copyright by

Xin Zheng

2012

ABSTRACT OF THE THESIS

Photothermal Nanoblade Delivery of Wild-type Mitochondria
into mtDNA Depleted Osteosarcoma Cells

by

Xin Zheng

Master of Science in Biomedical Engineering
University of California, Los Angeles, 2012
Professor Michael A. Teitell, Chair

Mitochondrial DNA (mtDNA) with deleterious mutations can cause severe inherited diseases due to defective energy metabolism. Studies have shown that mutated mitochondrial genomes alone are sufficient to cause diseased phenotypes in cells with wild-type nuclear genomes. This suggests that the transfer of mitochondria containing wild-type mtDNA into mutant cells may offer a way to rescue defective cell respiration. Several previous attempts to rescue diseased phenotypes using cell fusion have been either unsuccessful or irreproducible. Our development of a device called the photothermal nanoblade provides a new approach to rescue mtDNA defects. In this technique, a non-focused laser pulse is used to excite a titanium coating at the tip of a glass micropipette positioned adjacent to the membrane of a single cell.

The laser pulse creates an explosive vapor bubble in the surrounding aqueous cell medium that collapses in less than 1μs and which generates a shear force to cut an adjacent plasma cell membrane with high precision. Cargo, such as wild-type mitochondria, are then delivered through the hollow bore of the titanium tipped micropipette into the cell cytoplasm. This technique is, therefore, distinct from standard microinjection and can deliver large objects, such as mitochondria and intracellular bacterial pathogens, into recipient cells with minimal damage. The goal of this project is to improve the respiration defect of mtDNA-depleted osteosarcoma rho 0 cells by photothermal nanoblade delivery of wild-type mitochondria, and to validate by studying the resulting recovery in oxidative phosphorylation. We have isolated respiring yet uncoupled wild-type mitochondria from an engineered DsRedMito HEK293 line, and shown successful delivery into rho 0 cells with high efficiency, demonstrating the feasibility of photothermal nanoblade as a large cargo delivery tool. Data collected from multiple isolation-delivery experiments followed by media selection did not select a population with improved rho 0 respiration. A series of mitochondria characterization ruled out the possibility of mitochondrial autophagy, suggesting that chemiosmotic coupled isolated mitochondria could be the key to achieve cellular uptake of the delivered mitochondria.

The thesis of Xin Zheng is approved.

Pei-Yu Chiou

Daniel T. Kamei

Michael A. Teitell, Committee Chair

University of California, Los Angeles

2012

Table of Contents

1 Introduction ……1

1.1 MELAS syndrome as an example of mitochondria defect disease ……1

1.2 Mitochondrial DNA-depleted rho 0 cells as the recipient ……2

1.3 Photothermal nanoblade device principle ……4

1.4 Experimental procedure ……5

2 Materials and Methods ……8

2.1 143B TK-, rho 0 and DsRedMito cell culture ……8

2.2 Mitochondria Isolation ……8

2.3 Clark-type oxygen electrode measurement ……9

2.4 Rho 0 cell growth curve experiment ……10

2.5 Cell patterning protocol ……10

3 Results and Discussions ……12

3.1 Isolation of wild-type mitochondria ……12

3.1.1 MELAS wild-type cells as mitochondria donor ……12

3.1.2 DsRedMito HeLa cells as mitochondria donor ……12

3.1.3 DsRedMito HEK293 cells as mitochondria donor ……14

3.2 Characterization of isolated wild-type mitochondria ……15

3.2.1 Clark-type oxygen electrode measurement ……15

3.2.1.1 Whole cell respiration ……15

3.2.1.2 Isolated DsRedMito HEK293 mitochondrial respiration ……16

3.3 Characterization of the recipient rho 0 transcription factors ……20

3.4 Mitochondria delivery via photothermal nanoblade …… ……22

3.4.1 Dextran Rhodamine dye delivery ……22

3.4.2 Isolated wild-type mitochondria delivery ……23

3.4.2.1 Recipient cell viability ……23

3.4.2.2 DsRedMito mitochondria delivery with FM Green MitoTracker ……..…24

3.4.2.3 DsRedMito mitochondria with FITC-Dextran co-delivery …….....25

3.5 Post-delivery media selection ……...27

3.5.1 Rho 0 cell growth curve under uridine-free media selection ……...27

3.5.2 Selection experiment on injected rho 0 cells ……28

3.6 Post media selection colony isolation ……..32

3.6.1 Experimental injection plate ……..……32

3.6.2 Mitochondria dump control plate ……..……34

3.7 Immunofluorescence for LC3 autophagy marker ……36

4 Conclusion ……37

5 References ……..……39

1. Introduction

1.1 MELAS syndrome as an example of mitochondria defect disease

Mitochondrial DNA (mtDNA) with deleterious mutations can cause severe inherited diseases, such as mitochondrial myopathy, encephalopathy, lactic acidosis and stroke (MELAS) due to defective energy metabolism. MELAS syndrome is a progressive neurodegenerative disorder caused by defected mtDNA sequence. In the adult population of the United States, the frequency of MELAS is reported at about 16.3 patients per 100,000 individuals, and the life expectancy at the onset of symptoms is approximately five years (Singh et al. 2004). The MELAS disorder is known to be inherited maternally. This pattern of inheritance applies to genes contained in mtDNA, since egg cells, not sperm cells, contribute mitochondria to the developing embryo. Even though the syndrome can affect both males and females in every generation of a family, fathers do not pass mitochondrial traits to their children (Ciafaloni et al. 1992).

Genetic material within the mitochondria codes for proteins that help with mitochondrial energy production in cells throughout the body. Therefore, clinical presentations of MELAS can have multisystem involvement, including the central nervous system, skeletal muscle, eye, cardiac muscle, and the gastrointestinal system (Harano et al. 1994). Approximately 80% of MELAS syndrome cases are caused by an A to G point mutation in the dihydrouridine loop of transfer RNA ($tRNA)^{Leu\ (UUR)}$. This mutation causes misfolding of the affected tRNA, preventing the proper translation of UUR-rich proteins used in energy production, and giving rise to the syndrome. In order to understand whether the MELAS phenotype is caused by the mtDNA mutations alone or whether is dependent on a nuclear genome defect, *Hayashi et al*. performed

studies on clonal mtDNA-less HeLa fused with mutant mtDNA. The results suggested that mutations of mtDNA alone are sufficient to induce the mitochondrial dysfunction characteristics of the disease, independent of any nuclear genome defects (Hayashi et al. 1991). Such a discovery suggests that transfer of reparative wild-type mitochondria into mutant cells could potentially correct the defective respiration caused by the mutated mitochondria, thus improving the overall energy production and reducing the MELAS phonotype.

In past decades, several groups attempted to rescue respiration in MELAS syndrome cells. However, these experiments have been either unsuccessful or irreproducible due to, for example, a very low efficiency microinjection (King et al. 1988). Emerging interest in this subject encourages the usage of a more effective approach to achieve this goal.

1.2 Mitochondrial DNA-depleted rho 0 cells as the recipient

Recently the proposed experimental approach shifted from using MELAS mutant cells as the subject of rescuing respiratory function to using rho 0 cells, aiming for easier detection of delivered wild-type mitochondria incorporating into the endogenous defected mitochondria network. Rho 0 cells are mtDNA depleted cells that lack critical electron transport chain catalytic subunits. It is well-studied that 13 subunits of the mitochondrial oxidative phosphorylation (OXPHOS) enzyme complexes are encoded in the mtDNA located in the matrix of mitochondria (Wallace et al. 2005). Therefore, depletion of the mtDNA will deteriorate the cellular respiration, leading to inability to regulate redox potential and generate reactive oxygen species (Chandel et al. 1999). Although rho 0 cells contain petit mitochondria (since most of the proteins that make up mitochondria are encoded in nuclear DNA), they cannot rely on normal OXPHOS for energy

production, thus, they must survive and replicate using ATP derived solely from glycolysis (Chandel et al. 1999). The circular mtDNA genome also contains the mitochondrial rRNA genes and tRNA genes for local transcription and translation of these 13 subunits.

With the photothermal nanoblade injection of wild-type mitochondria containing intact mtDNA, the endogenous petit mitochondria of the rho 0 cells will theoretically fuse with the wild-type mitochondria in an effort to restore its OXPHOS activity. Over a certain period of culturing, successful cellular incorporation could recover the mitochondrial oxygen consumption level, which can be measured by the Seahourse machine as mentioned above. As opposed to the MELAS mutant cells, the rho 0 cells lack the mtDNA, making it easier to select and detect the influence of the incorporated wild-type mitochondria, as there will be no endogenous mtDNA to compete with the injected wild-type ones.

One of the greatest concern in our approach was whether the injected mitochondria and mtDNA would be significantly diluted as they fuse with the rho 0 petit mitochondria, and thus unable to show improved oxygen consumption. In 1992, Chomyn et al. had demonstrated increase in oxygen consumption level with as low as only 10% wild-type mtDNA introduced into the MELAS cells (Figure 1.), which gave positive outlook to our project.

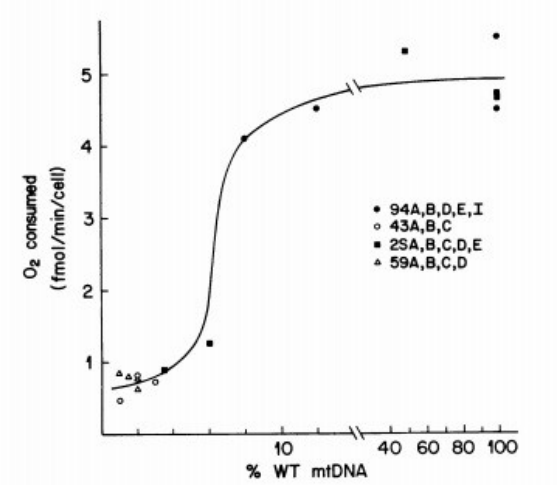


Figure 1. Approximately 10% of wild-type mtDNA can significantly improve oxygen consumption. (A. Chomyn et al. *Proc. Natl. Acad. Sci*.,1992, vol.89, pp.4221-4225)

1.3 Photothermal nanoblade device principle

Developed jointly with the Chiou research group, the photothermal nanoblade device provides a new method to deliver mitochondria into MELAS mutant cells. Figure 2 illustrates the principle of the photothermal nanoblade. First, a glass microcapillary pipette is coated with 200 nm titanium thin film before the experiment. Studies have shown that metallic nanoparticles adhered to cell surfaces can transiently porate the cell membrane for small molecule delivery upon pulse laser irradiation (Lapotko et al. 2006) and in this case, we adhere the metallic layer to a repositionable glass pipette. The laser pulse is generated by a Q-switched, frequency-doubled Nd:YAG laser operated at 532 nm wavelength and 6 ns pulsewidth. After passing through a series of beam splitters and lenses, the laser beam reaches the micropipette tip, heating the titanium coating. Immediately following the excitation, an explosive vapor bubble forms adjacent to the micropipette tip and collapses within 1 μs. The shear stress associated with the bubble explosion locally cuts the contacting cell membrane, and positive pressure applied to the solution loaded into the pipette injects cargo into the cell. The highly efficient membrane cutting

introduces only very limited mechanical perturbation to the rest of the fragile membrane (Wu at el. 2010). Photothermal nanoblade enables controllable membrane cutting and material delivery without physically advancing the micropipette into the cell, making it a less invasive membrane opening method compared to traditional microinjection.

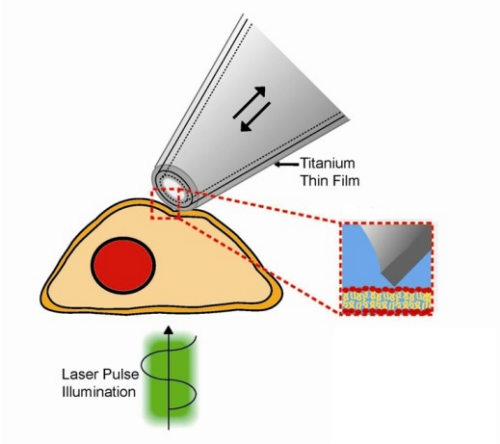


Figure 2. Principle of the photothermal nanoblade.

1.4 Experimental procedure

Figure 3 shows a schematic representation of the rho 0 or MELAS mutant phenotype mitochondria delivery experiment. Although rho 0 cells are chosen to be the recipient cell line in this study for simplicity and serve as proof of principle for this approach, our ultimate goal is to apply this technology to a model closer to real world clinical challenges, such as the MELAS patients. Therefore, the following schematic procedure denotes both rho 0 and MELAS mutant as the mitochondria recipient cell lines.

Approximately 3.5×10^7 DsRedMito cells, a HEK293 cell line with red fluorescent protein (RFP) labeled mitochondrial networks, are harvested to start the procedure. Cells are suspended

in a mitochondrial isolation buffer and protease inhibitor cocktail before homogenization. After dounce homogenization and a series of centrifugation steps, the collected mitochondria are either used to test respiration level with Clark-type oxygen electrode, or loaded into the micropipette for photothermal nanoblade injection.

Three plates of micro-patterned rho 0 cells are prepared for each mitochondria isolation-injection experiment. The small pattern allows better quantification of the mitochondria delivery efficiency and minimizes the percentage of un-injected cells in media selection period. (1) In the experimental plate, photothermal nanoblade injection was performed using the wild-type mitochondria isolated from DsRedMito cells. (2) In the mitochondria dump control plate, the isolated mitochondria are directly introduced and mixed into the media, bypassing the photothermal nanoblade delivery. (3) In the negative control plate, the rho 0 cells are simply maintained using the same media selection protocol as plate (1) and (2), without ever in contact with the isolated wild-type mitochondria

Confocal microscopy images are taken for all plates to provide evidence of the intracellular localization of the injected mitochondria inside recipient cells. Immediately after the photothermal nanoblade delivery, all three rho 0 plates are cultured for 14 days before changing to selection media. With a period of uridine-free selection media culturing, rho 0 cells that contained the delivered wild-type mitochondria will survive and form colonies. These selected rho 0 cells will be used for a series of biological assays to test for improved respiration. The two controlled rho 0 plates (2) and (3) are also tested in parallel with the experimental plate (1). We will also try to identify sequence the mtDNA in the injected cells using qRT-PCR. Based on the various assay readout, we can conclude whether the rho 0 respiration is improved by photothermal injection of wild-type mitochondria.

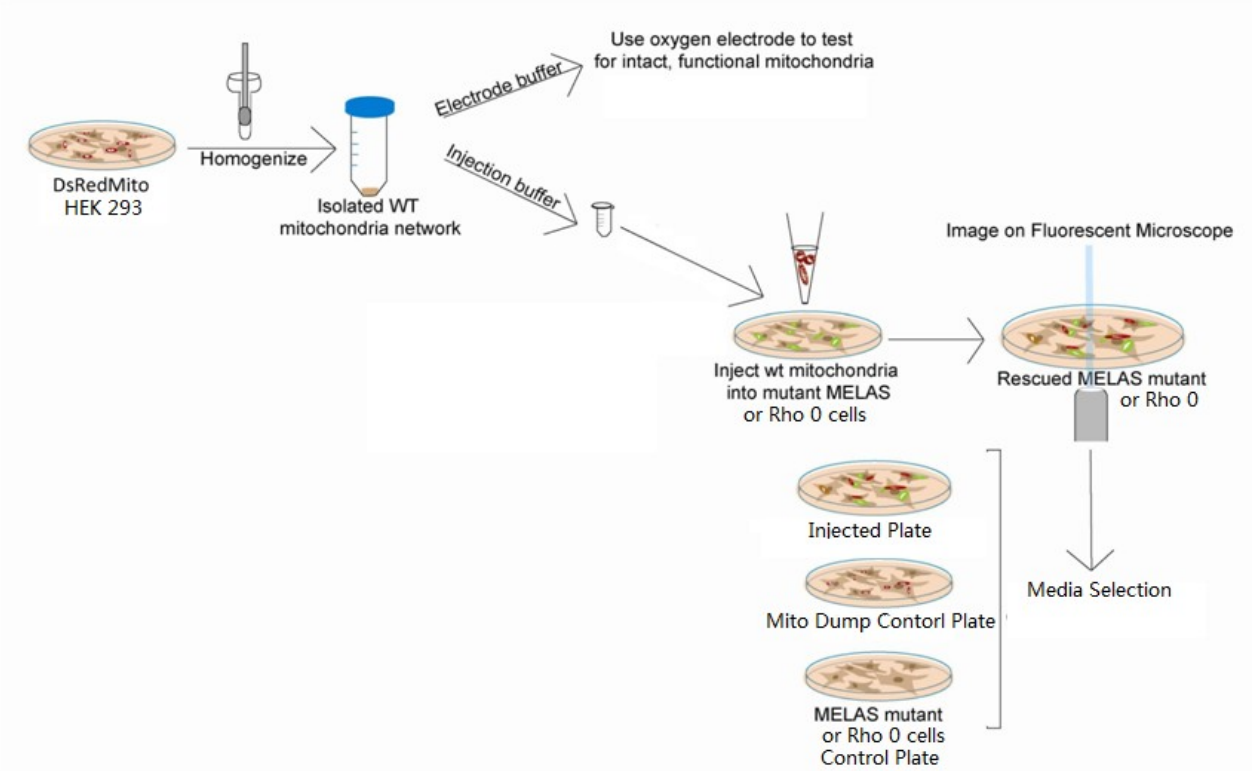


Figure 3. Schemetic procedure of the MELAS phenotype rescue experiment.

2. Materials and Methods

2.1 143B TK-, rho 0 and DsRedMito cell culture

The 143B TK- osteosarcoma parental line and its derived rho 0 cells were generously provided by Dr. Douglas C. Wallace. 143B TK-, rho 0 and DsRedMito cells were cultured on 10cm tissue culture dishes for passaging. When rho 0 cells were needed for photothermal nanoblade injection, they were then cultured on glass bottom plates to ensure imaging quality after injection. DsRedMito HeLa and DsRedMito HEK293 were maintained in complete Dulbecco's Modified Eagle Medium (DMEM) supplemented with 10% fetal bovine serum (Omega Scientific NC9868088), antibiotics (penicillin and streptomycin), glutamine, and non-essential amino acids. 143B TK- parental cells were cultured in the same complete media as DsRedMito HeLa except substituting glutamine with Q-max (Gibco 35050). The rho 0 cells were cultured on 143B TK- complete DMEM media with extra 0.05mg/mL uridine supplement.

2.2 Mitochondria Isolation

One confluent 15cm plate with about 3.5×10^7 DsRedMito HEK293 cells were harvested by trypsinization. After two washing steps using 10 ml ice cold PBS and centrifugation, the cell pellet was resuspended in 0.8 ml mitochondrial isolation buffer cocktail with 8 µl protease inhibitor. The sample was incubated on ice for 10 min before homogenization using a 2 ml dounce and tight-fitting pestle for 25 strokes. The broken cells were then centrifuged at 700g for 10 minutes at 4ºC and supernatant was collected. This step was repeated until very little lipid pellet was spun down. Then a high-speed centrifugation was used at 12,000g for 15 minutes to collect the mitochondria pellet. To wash off pro-apoptotic protein and improve recipient cell

viability, one important washing step is needed here with 0.8 ml isolation buffer and protease inhibitor cocktail. The resulting mitochondria pellet was resuspended in small volume (50 µl to 300 µl) of mitochondrial isolation buffer cocktail depending on the mitochondria yield. Sample was maintained at 4ºC before loading the photothermal nanoblade injection micropipette.

2.3 Clark-type oxygen electrode measurement

After carefully assembled the device, 50 µl of KCl electrolyte was added to connect the cathode and anode of the electrode. Liquid phase water calibration was chosen to set the zero oxygen consumption rate. An oxygen scavenger agent Na_2SO_3 was then added to consume all oxygen in water and calibrate zero oxygen level. After calibration, thoroughly wash the sample chamber with DI water. Measurements can start when electrical signal stabilized to about 2000 mV. If the signal is too late, consider adding more KCl electrolyte or reassemble the oxygen electrode.

The chamber was filled with 300 ml mitochondria isolation buffer when the sample was ready. The oxygen level in buffer was measured for 2 minutes before adding in 300 ml mitochondria sample. To avoid excess disturbance caused by sample loading, the sample was carefully introduced to the side-wall of the chamber. Four substrates (pyruvate, succinate, ADP and CCCP) were introduced to the mitochondria sample one by one and monitored the corresponding drop in oxygen level. To stimulate optimal respiration, the final concentrations of the four substrates are 8mM (pyruvate), 10mM (succinate), 50µM (ADP) and 0.3µM (CCCP) in the mitochondria sample.

Post-measurement analysis was performed based on the oxygen level plot obtained from Clark-type oxygen electrode. The slope of the trace following the addition of each substrate indicates the rate of oxygen consumption. The functionality and intactness of the isolated mitochondria can therefore be estimated by comparing different levels of respiration rate with different substrate

2.4 Rho 0 cell growth curve experiment

Two six well plates were used for the selection experiment. One plate was plated with rho 0 cells while the other was plated with 143B TK- cells. The cells were plated at a low concentration to make sure that they would not overgrow in the 6 day experiment period. 24 hours after initial plating, both six well plates were changed to uridine-free selection media made from dialyzed FBS. Starting day 0, the total amount of cells in each plate will be counted each day, with flow cytometry experiment to confirm the cell death in the two population.

2.5 Cell patterning protocol

Rectangular glass cover slips were soaked in 0.1M NaOH for 15 minutes then rinsed with water and air dried. One drop of 5% (w/v) solution of PVA was placed onto one slide and sandwiched with another slide to evenly spread the PVA. Slides were placed on hotplate at 140 ºC overnight and later washed thoroughly with ethanol and water. Using the micromanipulator from the photothermal nanoblade set up, precise patterns were created on the slides using NaOCl. Lastly, slides were dipped in 1M HCl to remove NaOCl and washed with DI water.

PDMS was cured and cut into a rectangular wall the size of the PVA coated glass slides. The walls and the glass cover slips were glued together with additional PDMS and cured for at least 1-2 hours. 10^4 rho 0 cells are then seeded into these wells. After incubating the cell for around 12 hours, certain cells attach and grow in the circular patterned area without PVA coating, other cells will die and float in the media. By simply replacing the media, the dead cells were washed away and the plate is ready for photothermal nanoblade injection of isolated DsRedMito mitochondria sample.

3. Results and Discussions

3.1 Isolation of wild-type mitochondria

3.1.1 MELAS wild-type cells as mitochondria donor

MELAS wild-type cells were initially selected as the mitochondria donor to be delivered into MELAS mutant cells. In order to visualize and distinguish between delivered and endogenous mitochondria under florescence microscope, the wild-type mitochondria were stained with MitoTracker prior to isolation. While both the CMXRos Red and FM Green MitoTracker showed promising mitochondria labeling in live cells, the fluorescence signal was lost after a series of washing and centrifugation steps during isolation. Therefore, the approach of using MitoTracker to label different mitochondria source in downstream experiment was ineffective. A new donor line with fluorescence protein modified mitochondria is desired in order to track the delivery of wild-type mitochondria *in vivo*.

3.1.2 DsRedMito HeLa cells as mitochondria donor

The DsRedMito HeLa was then chosen as mitochondria donor because they contain RFP expressing mitochondria which can provide visual evidence of successful delivery into recipient cells. DsRedMito HeLa is engineered via viral infection of a DsRedMito plasmid vector which contains the sequence for an RFP protein. RFP is fused with a mitochondrial localization sequence (MLS). This RFP-MLS gene is stably incorporated into nuclear genome and is transcribed and translated with the rest of the HeLa genome. Lastly, MLS facilitates the transportation of RFP into the mitochondria matrix.

The isolation using an optimized mitochondria isolation protocol was performed with DsRedMito HeLa. The donor cells and mitochondria involved in this process were carefully maintained at 0°C on ice to minimize cellular kinetic activity. Figure 4 shows two fluorescent images of the DsRedMito HeLa mitochondria, in both live cell and isolated form. The left image illustrates mitochondria networks in its native morphology inside cells. The right image shows the same DsRedMito mitochondria after isolation procedure. Notice the similar shape of the scattered red fluorescent signals in these images compared to mitochondrial imaged inside a cell. Negative controls show no fluorescent signals under when imaged.

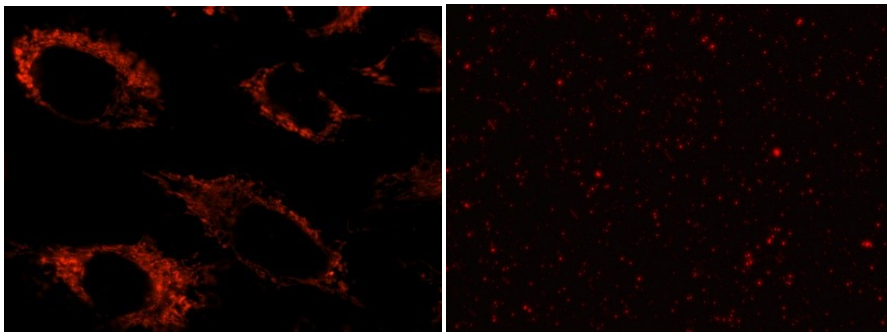


Figure 4. Left: Cultured DsRedMito HeLa live cells. Right: Isolated DsRedMito HeLa mitochondria.

Although isolated DsRedMito HeLa mitochondria showed promising fluorescence signals and cluster shape morphologically, we were only able to collect a barely visible size of mitochondria pellet at the end of isolation using 3.5×10^7 cells. Such small yield not only complexes the downstream delivery process, but also makes it impossible to prepare a high enough mitochondria concentration for oxygen electrode measurement, which is critical in evaluating the quality of the isolated mitochondria. The functionality of the isolated mitochondria is the fundamental criterion to achieve the goal of improving defected respiration. For that reason, the DsRedMito HeLa is not the most ideal wild-type mitochondria donor.

3.1.3 DsRedMito HEK293 cells as mitochondria donor

Approximately 3.5×10^7 HEK293 cells were used to perform a preliminary isolation experiment, resulting in a mitochondria pellet of desirable size (5mm radius). The pellet was then re-suspended in isolation buffer and measured its oxygen consumption rate with the Clack-type oxygen electrode. Since the preliminary oxygen electrode data showed promising respiration of the isolated mitochondria from HEK293 cells, we performed viral transduction using DsRedMito plasmid and generated a new DsRedMito HEK293 line with RFP labeled mitochondria. DsRedMito HEK293 is the most commonly used wild-type mitochondria donor in this project. Data exhibiting the activity and respiration of these isolated mitochondria will be discussed in the following session.

3.2 Characterization of isolated wild-type mitochondria

3.2.1 Clark-type oxygen electrode measurement

3.2.1.1 Whole cell respiration

The Clark-type oxygen electrode was used as an important metric to assess the respiration capacity of cells as well as functionality of isolated wild-type mitochondria. The Clark electrode measures oxygen on a catalytic platinum surface using the net reaction:

$$O_2 + 4\ e^- + 2\ H_2O \rightarrow 4\ OH^-$$

The reduction reaction allows a current to flow; this creates a potential difference which is recorded on a flatbed chart recorder. The current flowing is proportional to the activity of oxygen in a well-stirred sample solution. In oxidative phosphorylation of the mitochondria energy metabolism, as electron passes down the electron transport chain (ETC), oxygen serves as the final electron acceptor, driving the above reaction. Therefore, the oxygen electrode trace output is a measure of the oxygen activity of the sample.

Before moving to measuring oxygen consumption of the isolated wild-type mitochondria, we first collected respiration data on the whole-cell level for four potential mitochondria donor and recipient cell lines. Figure 5 shows very robust respiration in DsRedMito HeLa and 143B TK- osteosarcoma cell lines. The 143B TK- derived rho 0 cells have respiration level the same as the buffer, confirming the rho 0 characteristic of defected oxidative phosphorylation and nonfunctional electron transport chain. HEK 293T cells have an oxygen consumption rate in between of rho 0 and the 143B TK- parents, representing effective oxidative phosphorylation and its potential to be used as wild-type mitochondria donor.

From Figure 5, DsRedMito HeLa might seem to be a better candidate as wild-type mitochondria donor. However, as mentioned above, the limited mitochondria yield prevented us from using oxygen electrode to evaluate its respiration functionality post isolation. The higher mitochondria yield of HEK293 cells, on the other hand, allows reproducible and robust measurement of its respiration. This leads to the final decision of using DsRedMito HEK293 as wild-type mitochondria donor.

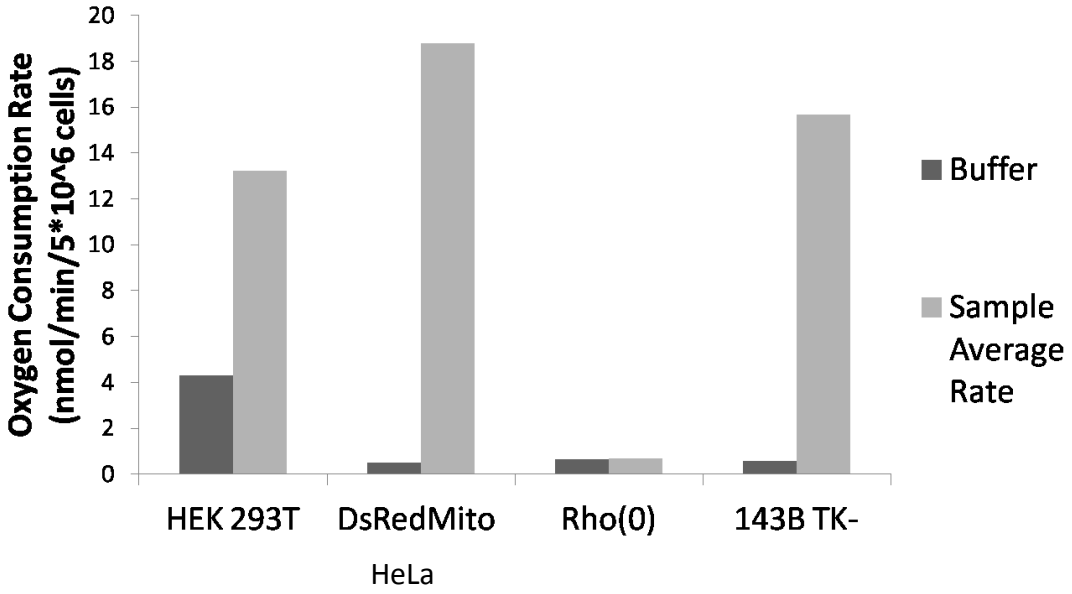


Figure 5. Average oxygen consumption rate of HEK293, DsRedMito HeLa, rho 0 and its parental 143B TK- cells. Oxygen electrode measured whole cell respiration in this experiment.

3.2.1.2 Isolated DsRedMito HEK293 mitochondrial respiration

The isolated DsRedMito HEK293 mitochondria have shown consistent respiration and oxygen consumption based on multiple oxygen electrode measurements (n=8). Data also suggests that the isolated mitochondria lose their proton gradient coupling effect, which is a measurement of mitochondrial intactness.

To assess the respiration level of wild-type mitochondria after isolation, DsRedMito HEK293 cells were homogenized by 25 strokes with a 2 ml dounce homogenizer and tight-fitting pestle. One example of the 8 isolated mitochondria oxygen consumption measurements is shown in Figure 6

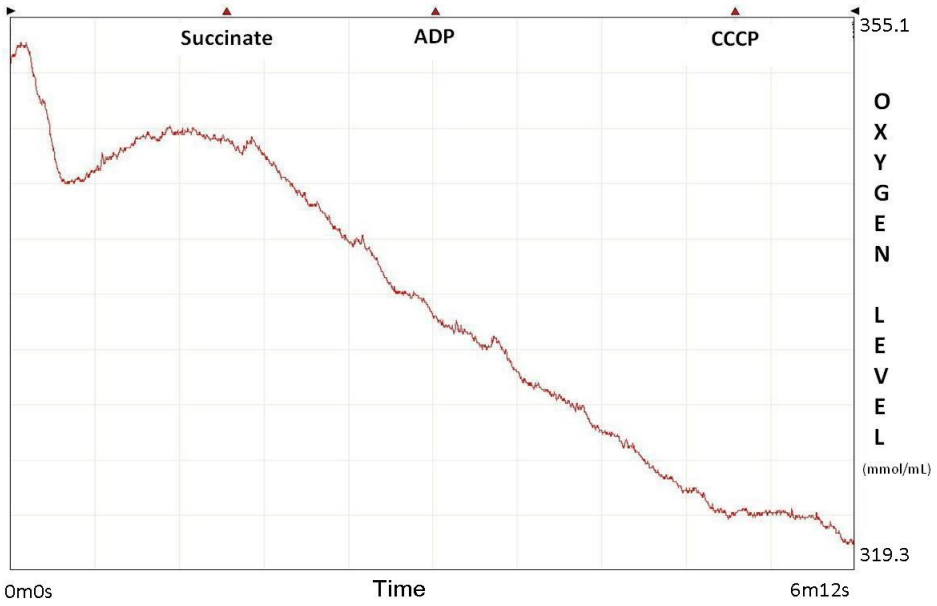


Figure 6. Clark-type Oxygen Electrode readout on HEK293 isolated mitochondria. Oxygen level (mmol/ml) was plotted versus time (min).

In Figure 6, the overall descending plot shows oxygen consumption over a period of time. The initial rapid drop in oxygen level can be accounted by the loading of the mitochondria sample. After the initial disturbance, the recording was stabilized to a constant level, and a mitochondria substrate, succinate, was added into the system. Immediate response to succinate was observed as the oxygen level decreased. A similar negative slope was found with introduction of adenosine diphosphate (ADP). Finally, when carbonylcyanide-m-chlorophenylhydrazone (CCCP) was added, no further oxygen consumption as it stabilized around 321 mmol/ml for the remaining time.

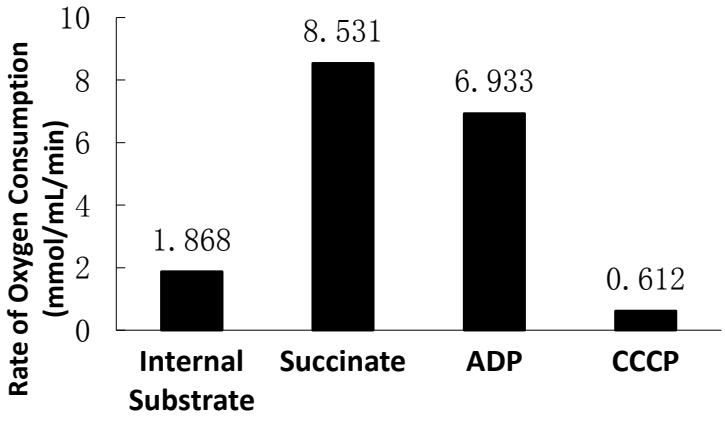


Figure 7. Rates of Consumption when different substrates were added. Slope data were extracted from the oxygen electrode plot in Figure 6.

We can conclude from the above results that even though the electron transport chain is functioning and consuming oxygen, the proton coupling of oxidative phosphorylation seemed lost due to probably the disruption of mitochondrial outer membrane. In the electron transport chain of intact mitochondria, the oxidative phosphorylation is coupled. The substrates to be oxidized (e.g. succinate) donate protons and electrons to electron transport chain. As the protons are being pumped out from matrix to intermembrane space, the electrons are transported through the electron transport chain, and eventually accepted by the oxygen molecules. The influx of protons through ATP synthase back to the matrix drives the production of ATP from ADP. The oxidative phsophorylation is coupled only when the mitochondria membrane potential is intact (Hatefi, 1985).

Succinate, being one of the mitochondria substrates, was consumed when added, which indicates the functionality of the electron transport chain complex I to IV. However, in intact mitochondria, we would expect to see a higher rate of oxygen consumption with ADP than succinate in Figure 7, because of the coupling effect. We assume the internal ADP is completely

consumed, so when ADP was added from outside, it should drive the proton gradient and further stimulate the state 3 oxygen consumption (Hatefi, 1985). However, as described above, we did not observe such a coupling effect. This can be interpreted as the lost of membrane potential, which is caused by the disruption of outer membrane during isolation. Similarly, CCCP completely dissipates mitochondrial membrane potential, which would stimulate maximum oxygen consumption. Again, no coupling can be seen from Figure 7, suggesting these mitochondria were not coupled.

Figure 8 below shows another Clark-type oxygen electrode measurement. From the higher slope value, we can see a more robust oxygen consumption rate throughout this trial compare to the previous one shown in Figure 7. Such changes can be accounted by improved mitochondrial isolation technique and variation of the mitochondrial sample concentration. Nevertheless, the relatively lower level of oxygen consumption with ADP and CCCP compare to succinate is still consistent with the previous discussion.

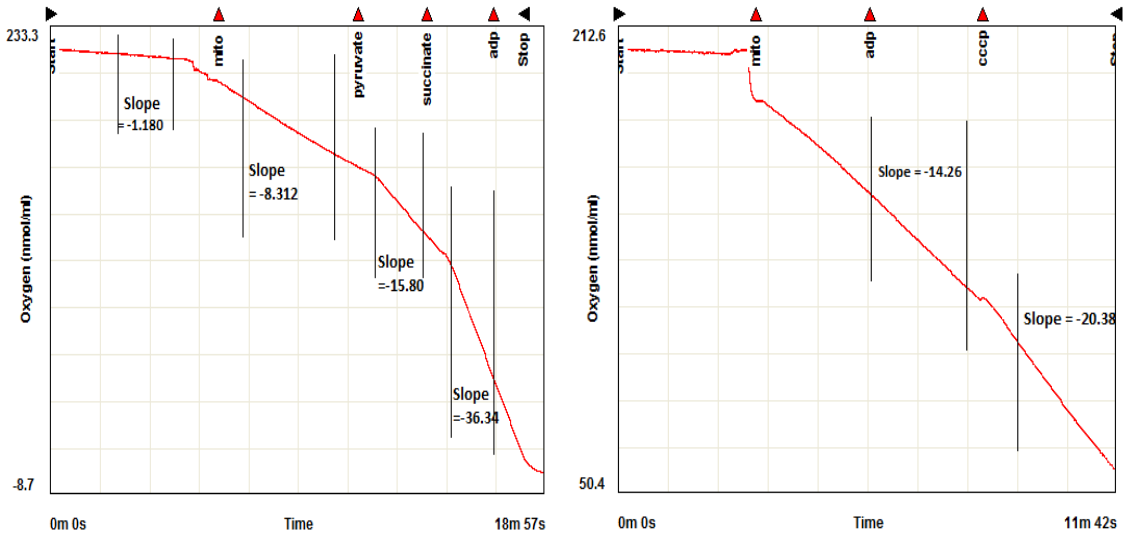


Figure 8. DsRedMito HEK293 isolated mitochondria oxygen consumption

3.3 Characterization of the recipient rho 0 transcription factors

Choosing the 143B TK- derived rho 0 cells as the wild-type mitochondria recipient line is advantageous because they have a clean mtDNA background that allow us to detect any delivered mtDNA easily. However, since rho 0 cells lack mtDNA, it may also cause down-regulation or even deactivation of some mtDNA specific transcription factors. In this project, the goal of improving rho 0 defective respiration requires successful transcription and translation of the delivered mtDNA, making these mtDNA specific transcription factors extremely important. To test for the expression level of four transcription factors, we performed quantitative real-time PCR (qRT-PCR). The data is shown in Figure 9.

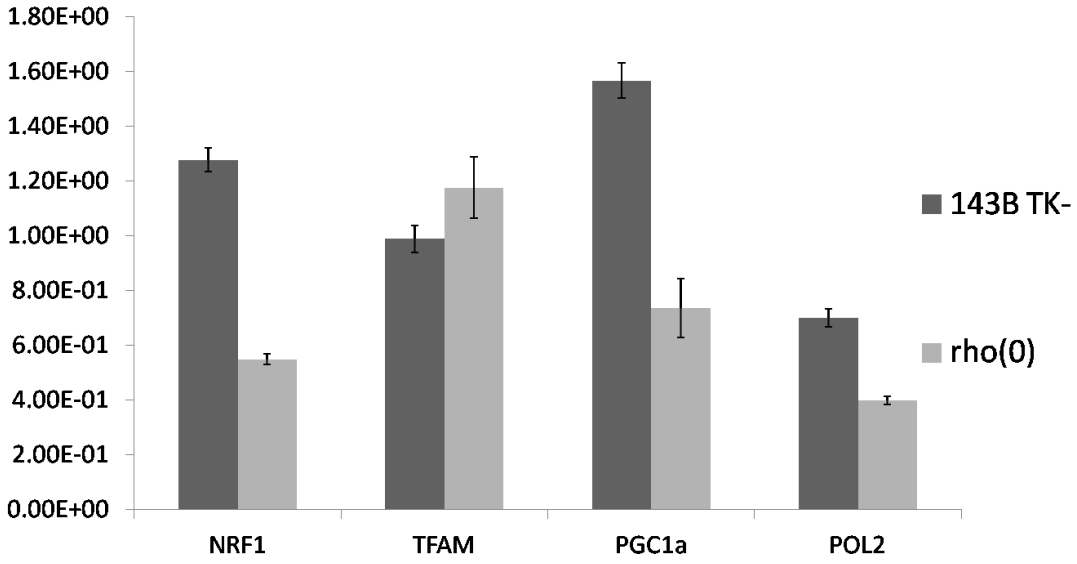


Figure 9. qRT-PCR for rho 0 transcription factor expression levels.

According to Figure 9, rho 0 still maintains reasonable level of each transcription factors. NRF1 and PGC1α are transcription co-activators of nuclear-encoded mitochondria proteins important in energy metabolism. TFAM is a mtDNA-specific transcription factor and plays a key

role in mtDNA transcription. POL2 is responsible for mtDNA replication. Other than TFAM, the expression levels of NRF1, PGC1α and POL2 in the parental 143B TK- cells are higher than rho 0 cells. Although expressed at a lower quantity, the data suggests that rho 0 still have a moderate amount of mitochondria transcription specific proteins despite having no mtDNA. These important genes do not seem to be turned off. This piece of data is critical since it provides positive evidence to support our approach at the biomolecular level.

3.4 Mitochondria delivery via photothermal nanoblade

3.4.1 Dextran Rhodamine dye delivery

As a proof-of-principle of the photothermal nanoblade live cell membrane cutting ability, a titanium-coated microcapillary pipette was loaded with a membrane impermeable fluorescent dye Dextran-Rhodamine. After initial focusing on the nucleus of the cell, the focus plane is slightly readjusted above the cell surface, preventing occasional breakage of the micropipette tip due to errors in operating the device. The micropipette tip was then brought into light contact with the cell membrane, giving rise to a slight change in cell shape as a result of the contacting pressure exerted by the tip. Immediately after laser pulsing at 150 mJ/cm^2, the dye molecules were injected into the cell. The cell membrane opening by photothermal nanoblad is verified by the Rhodamine dye delivery into the cells shown in Figure 10.

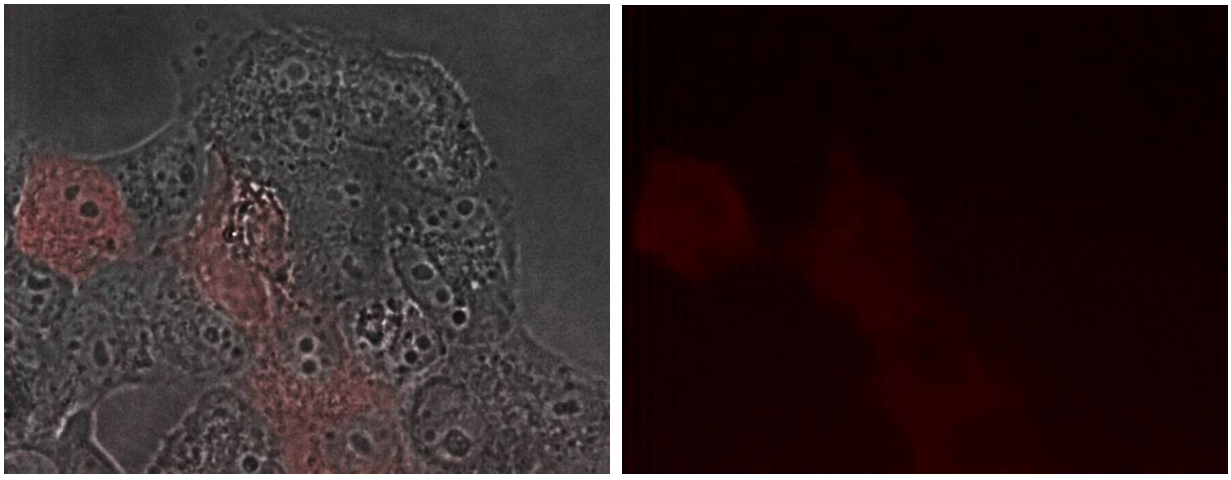


Figure 10. Photothermal nanoblade injection of dye into live cells. The inner diameter of the micropipette was 1.4um.

3.4.2 Isolated wild-type mitochondria delivery

3.4.2.1 Recipient cell viability

Following our initial mitochondria isolation protocol, the final mitochondria pellet was collected and re-suspended in isolation buffer containing FITC-dextran co-injection dye. Repeated experiments indicate that the rho 0 recipient cells died rapidly after the photothermal nanoblade delivery. For example, in one trail which we injected mitochondria into approximately 80 cells, only one or two cells stayed alive (or maintaining their FITC-Dextran signal) 24 hours after. Two reasons can be accounted for the loss of FITC-Dextran labeling in rho 0 cells: (1) apoptosis releases FITC from the cytosol; (2) gradual diffusion and decreased fluorescent intensity of FITC. We recognize that counting the number of green cells 24 hours later as a measurement to estimate recipient cell viability might not be a very accurate approach since a lot of factors, such as cell division, FITC diffusion and degradation, can affect the cell count. Nevertheless, it provides a good reference that we can use to estimate the viability of rho 0 cells. The equation to calculate recipient cell viability after photothermal nanoblade delivery is shown below,

$$Recipient\ Cell\ Viability = \frac{Number\ of\ green\ fluorescence\ cells\ 24hrs\ post\ delivery}{Number\ of\ green\ fluorescence\ cells\ 2hrs\ post\ delivery} \times 100\%$$

In order to identify the cause of such drastic cell dead after wild-type mitochondria delivery, we first tested for the effect of laser pulse energy used in photothermal nanoblade delivery to rho 0 cells. One of the advantages of photothermal nanoblade is its capability of having high recipient cell viability post delivery, and this has been shown in previous published papers (French et al 2011). With a series of data collected to find a laser energy that is both with high membrane cutting efficiency and cell survival rate, we concluded that the rho 0 cell specific

optimum laser pulse energy to be around 90 μJ. This is about two folds less than the injection energy density used for HeLa, which is more robust than rho 0 cells. In addition, with only the isolation buffer loaded and delivered, the rho 0 cell viability was 80% 24 hours later. It is clear that it was some components in the isolated mitochondria sample that caused rho 0 cell death. When a cell is disrupted in the isolation process, pro-apoptotic proteins, such as cytochrome c, can be released and mixed with the isolated sample. It is known that cytosolic cytochrome c released from mitochondria can initiate the apoptotic program (Yang et al. 1997), which correspond to what we observed in our experiments.

Indeed, the rho 0 recipient cell post delivery viability dramatically increased from approximately 2% to 60% with an additional washing using 0.8 ml of mitochondria isolation buffer/protease inhibitor cocktail. The washing further diluted the concentration of the pro-apoptotic protein, making the final isolated mitochondria sample pure and easier for rho 0 cells to tolerate.

3.4.2.2 DsRedMito mitochondria delivery with FM Green MitoTracker

After resolving the recipient cell viability problem, we started the actual wild-type mitochondria isolation and delivery experiment. The rho 0 cells were first stained with FM Green Mitotracker to label the rho 0 cell endogenous mitochondria before injection. After delivery of the DsRedMito, two additional PBS washes were used to wash off the DsRedMito RFP units floating extracellularly in the media before confocal imaging. The confocal microscopy image in Figure 11 gives evidence of successful photothermal injection of DsRedMito mitochondria.

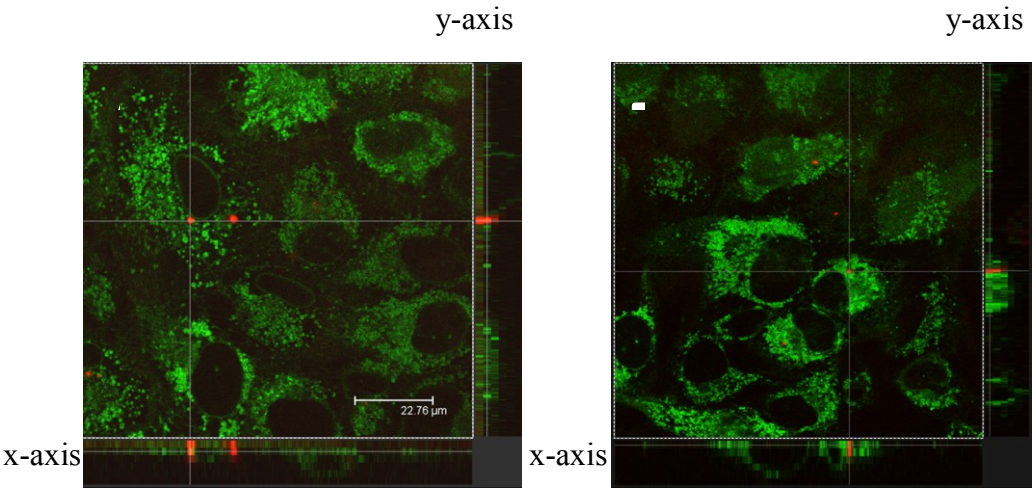


Figure 11. Injection of isolated DsRedMito mitochondria into rho 0 cells labeled with FM Green MitoTracker.

Figure 11 shows rho 0 cells that contains DsRedMito RFP units imaged at the same x-, y-, and z-plane as detected by confocal microscopy. According to the x and y cross-section in the images, the DsRedMito RFP units are surrounded by green rho 0 petit mitochondria. This kind of localization confirms that the delivered DsRedMito RFP units are indeed inside the recipient cells. In addition, our 2X washing step also minimized the chance of excess RFP units in media.

3.4.2.3 DsRedMito mitochondria with FITC-Dextran co-delivery

Although MitoTracker FM Green successfully stained rho 0 endogenous mitochondria, it is not designed for long-term culturing of the stained sample. But in our experiment, downstream culturing is critical after the initial mitochondria delivery and imaging. Therefore FITC-Dextran replaced MitoTracker to serve the purpose of labeling recipient cells and allow tracking of their viability. In each full experiment, the FITC-Dextran is dissolved in the standard isolation buffer/protease inhibitor cocktail and co-delivered with mitochondria into rho 0 cells. A confocal image is taken after delivery to confirm the location of the mitochondria within recipient cells.

Approximately 24 hours post delivery, another set of fluorescence images are collected to determine recipient cell viability as well as mitochondria delivery efficiency by counting the number of green fluorescent cells and red DsRedMito units within them.

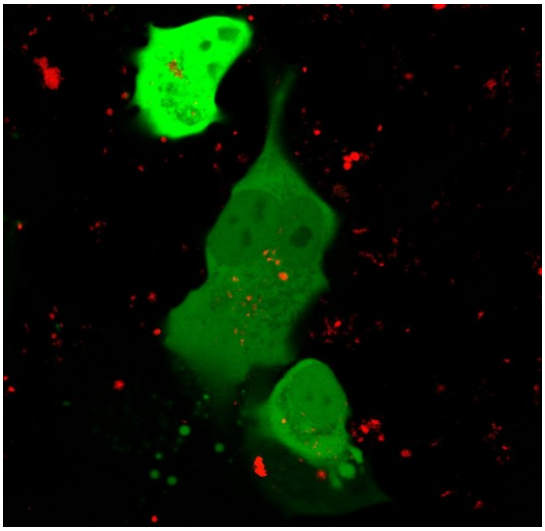


Figure 12. shows a confocal image of rho 0 cells after DsRedMito HEK293 mitochodnria delivery.

Figure 12 shows a confocal image of rho 0 cells 2 hours after mitochondria delivery. We can clearly see DsRedMito RFP units scattered thuroughout the rho 0 cytoplasm. Confocal images are taken at the same x and y plane, thus we can conclude again that the delivery is successful and the wild-type mitochondria are indeed within rho 0 cells. Extracting data from multiple confocal images similar to Figure 12, we fount the average DsRedMito RFP-mitochondria units delivery efficiency is about 3.67 units/cell, with standard deviation of 0.98. Despite the relatively low number, we theoretically only need 10% of wild-type mtDNA to improve oxygen consumption according to Chomyn et al (1992). In addition, the size of each RFP units also varies. This suggests that the current concentration of injected RFP units can potentially have an effect on the rho 0 cell oxygen consumption.

3.5 Post-delivery media selection

3.5.1 Rho 0 cell growth curve under uridine-free media selection

Figure 13 shows the growth curve of rho 0 cells growing in their normal uridine-rich media and in "uridine-free" selection media (containing non-dialyzed FBS from Omega Scientific NC9868088) respectively. The growth rate of the two populations were similar for the first four days, until the drastic decrease in the uridine-free selection population observed in Day 5. On Day 2 and Day 4, the rho 0 cells were stained with Annexin V and PI, then analyzed by flow cytometry. The result did not show significant difference in cell death between the cells under uridine-rich and uridine-free media, which is consistent with the growth curve shown in Figure 13.

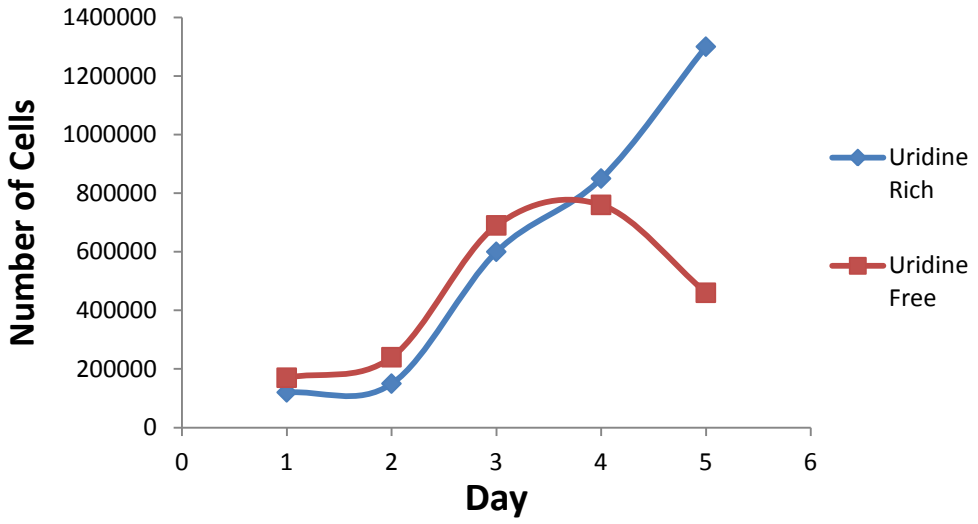


Figure 13. Rho 0 growth curve in uridine-rich and uridine-free selection media. A drastic decrease in cells under uridine free media took place between Day 4 and Day 5.

According to the selection experiment, it takes about five days for the selection to show effect. The decreasing rho 0 cell population under uridine-free selection fits our prediction, since rho 0 cells require uridine to survive. Rho 0 cells depend on pyrimidines because dihydrooratate

dehydrogenase, an enzyme in the pyrimidine biosynthetic pathway, is located in the mitochondrial inner membrane and requires mitochondrial electron transport for normal function (Gregoire et al. 1984). Rho 0 cells cannot synthesize uridine because they do not have mtDNA to produce major proteins in the electron transport chain. Therefore, the cells cannot replicate and expect to die within 5 days without uridine supplement. Note that the normal FBS (Omega Scientific NC9868088) we used to make complete media might contain some uridine, so even without additional supplement, the regular complete media (same as the uridine-free media) might have small amount of uridine.

To avoid such risk, we ordered a carefully dialyzed FBS (Hyclone #SH30079.02) to make the uridine-free media. Substances with molecular weight smaller than 10,000 are removed by dialysis in this special FBS, eliminating any uridine residue.

In summary, three types of growth media are involved in the selection process: (1) Complete media with Omega Scientific FBS (may contain small amount of uridine); (2) Complete uridine-free media with Dialyzed Hyclone FBS (contain no uridine); (3) Uridine-rich media (contain 0.05mg/mL uridine supplement).

3.5.2 Selection experiment on injected rho 0 cells

After proving successful delivery of isolated mitochodnria into rho 0 cells by confocal microscopy, we performed 11 sets of photothermal nanoblade injection experiments with the intention to maintain the culture and select for the successfully delivered recipient cells. Three plates of rho 0 cells were prepared in each of these sets: (1) In the experimental plate, photothermal nanoblade injection was performed using the wild-type mitochondria isolated from

DsRedMito cells; (2) In the mitochondria dump control plate, the isolated mitochondria are directly introduced and mixed into the media, bypassing the photothermal nanoblade delivery; (3) In the negative control plate, the rho 0 cells are simply maintained using the same media selection protocol as plate (1) and (2).

Immeidately after mitochondria delivery, the rho 0 were allow to grow for 14 days under their regular uridine-rich media. This period allows the cells to recover from delivery and expand to a larger population. More importantly, this also gives enough time for mitochondria fusion and restoration of their respiratory enzyme activity (Ono et al. 2001). On the 15th day, we removed the addition uridine supplementn and started culturing all three plates in complete media with non-dialyzed FBS. As mentioned in the previous session, such FBS contained small amount of uridine, therefore, serve as a cushion /buffer before we swtich to completely uridine-free media 2 weeks later. Finally, 4 weeks after delivery of wild-type mitochondria, all three plates were switched to the uridine-free selection media made from dialyzed FBS. A significant drop in cell confluency was observed in all plates, as shown in Figure 14.

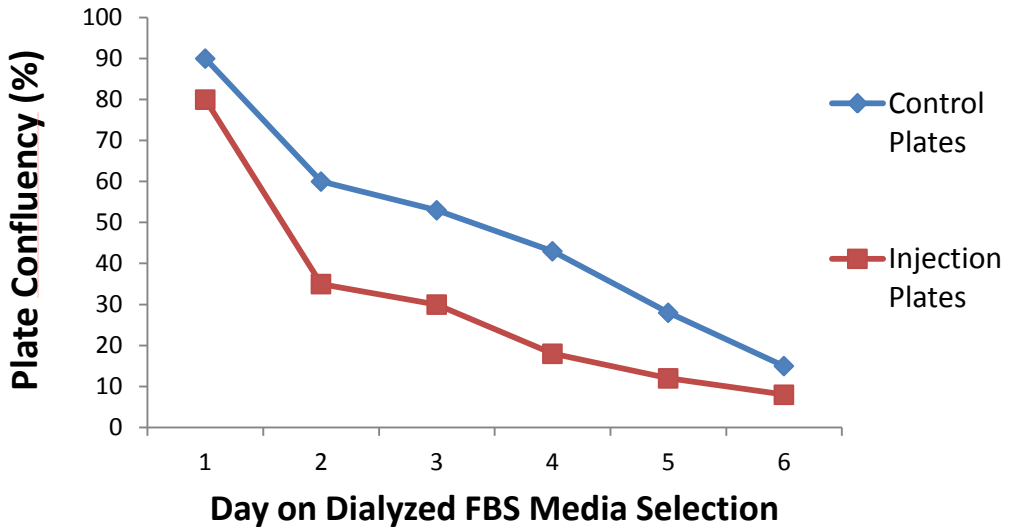
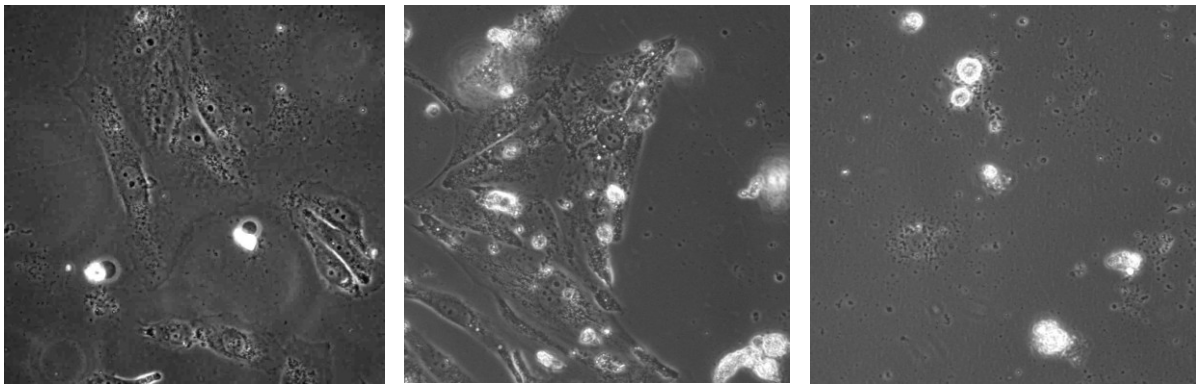


Figure 14. Example of one 1/20/12 Dialyzed FBS Media Selection

Figure 14 is an example of rho 0 cell confluency under uridine-free media selection. Both the control rho 0 plate and the experimental injection plate experienced drastic decrease in cell population within a week. Their confluency droped from 80% - 90% to eventually under 10%. By the end of the three weeks uridine-free selection period, we noticed that about 5% of cells still attached to the cell culture plate including those in the negative controls, which we expected them to die out completely. These 5% cells had a larger, flatten morphology and no cell division, which assembled characteristics of senescence cells. All of the 11 photothermal nanoblade mitochondria delivery followed this similar trend of decreasing rho 0 population when undergoing uridine-free selection media.



Injection Plate Control Plate Control Dump Plate

Figure 15. Images taken from one of the photothermal nanoblade delivery experiment under uridine-free media selection.

Figure 15 provides images of rho 0 cells 5 days after uridine-free media selection. Cell confluency in the experimental injection plate and the control rho 0 plates all decreased and floating dead cells can be seen in both images. We can see in this particular mitochondria delivery experiment that cells in the control mitochondria dump plate were all dead. This is not commonly found in other 10 mitochondria delivery experiments. The majority of control dump

plates from other trials maintained at 5% confluency similar to others. As we will discuss in later session, some colonies actually grew from the control mitochondria dump plates.

The rho 0 cells are cultured in the uridine-free media with Dialyzed FBS for 3 weeks, and we observed no further decrease in cell population by the end. We switch the selection media back to complete media with small amount of uridine (Omega Scientific FBS) since the dialyzed FBS from Hyclone eliminates all substances smaller than 10,000MW and was not designed for long-term culturing.

3.6 Post media selection colony isolation

3.6.1 Experimental injection plate

After the uridine-rich→ minimum uridine → uridine-free media selection scheme, the cells were put back to minimum uridine-containing media for long term culturing. Soon after switching back to the moderate growth environment with small uridine supplement, we noticed that some of the rho 0 cells still attached to the plate started to divide and grow again. Within 2 weeks, these dividing cells have formed small colonies, or proliferation centers, to the size visible by human eyes.

We identified about 3-5 proliferation centers/colonies per experimental mitochondria injected plate, making a total of roughly 25 rho 0 proliferation centers found in all 11 experiments. Figure 16 shows two adjacent proliferation centers imaged over a course of 3 days. It is clear from the figure that both the radius and the density of the two proliferation centers increased over time, suggesting that these rho 0 cells survived the harsh uridine-free selection process and maintained cell growth ability.

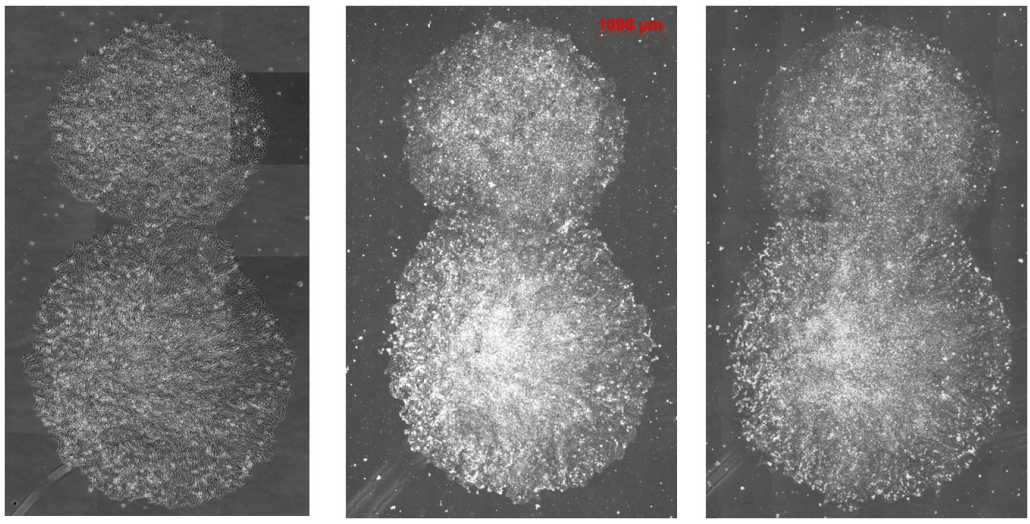


Figure 16.Injection plate from one of the mitochondria delivery experiments. Post media selection (Characterized-Dialyzed-Characterized). Colonies growing over a course of three days.

Almost two months since the isolated mitochondria delivery, we obtained qualitative data showing colonies growing out from the injection plate. To further investigate whether these rho 0 colonies contain the delivered wild-type mtDNA, we performed qRT-PCR using cells collected from the colonies. Data is shown in Figure 17

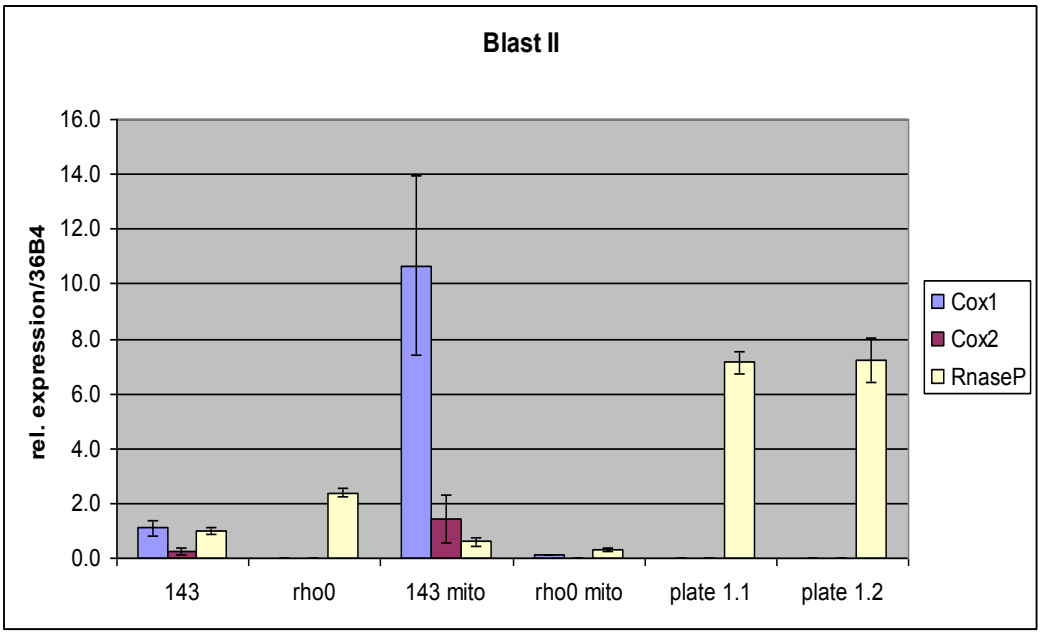


Figure 17. Quantitative Real-Time PCR to detect COX1, COX2 and RNase P expression in 143B TK- cells, rho 0 cells, 143B TK- mitochondria, rho 0 mitochondria and the colonies from plate 1.1, plate 1.2. Note that 143, rho0, plates 1.1 and 1.2 RNA were prepared from whole cells.

In Figure 17, Plate 1.1 and Plate 1.2 are cells collected from the two proliferation centers. 143, rho 0, Plate 1.1 and Plate 1.2 RNA were prepared from whole cells, while 143 mito and rho 0 mito RNA were collected from isolated mitochondria. Here we quantified expression levels of the mtDNA-encoded Cytochrome c oxidase COX1, COX2 and compared with nuclear-encoded RNase P. Result shows that rho 0 cells only have expression of the nuclear-encoded RNase P but no COX1 and COX2 due to its lack of mtDNA. Unfortunately, data also indicates that there is no COX1 and COX2 expression in Plate 1.1 and Plate 1.2 cells either, leading to the conclusion that no wild-type mtDNA was integrated by the rho 0 cells from proliferation centers. These rho 0

cells' ability to survive such harsh uridine-free selection for almost 3 weeks was unexpected. It seemed that they regained their cellular function and resumed cell division once a small source of uridine was introduced by the end of the selection. The mechanism behinds such behavior is unknown and requires future research to understand it.

3.6.2 Mitochondria dump control plate

One of the controls we have in this photothermal nanoblade mitochondria delivery experiment was the mitochondria dump plate, in which the isolated mitochondria are directly introduced and mixed into the media, bypassing the photothermal nanoblade delivery. The isolated mitochondria were incubated with the rho 0 cells overnight and then washed off.

The same media selection scheme was used for the mitochondria dump plate along with the experimental injection plate. However, by the end of the selection process, we not only found proliferation centers rising from the injected plates as mentioned in last session, but also observed colonies from the mitochondria dump control plates. Figure 18 shows two of these control plate colonies.

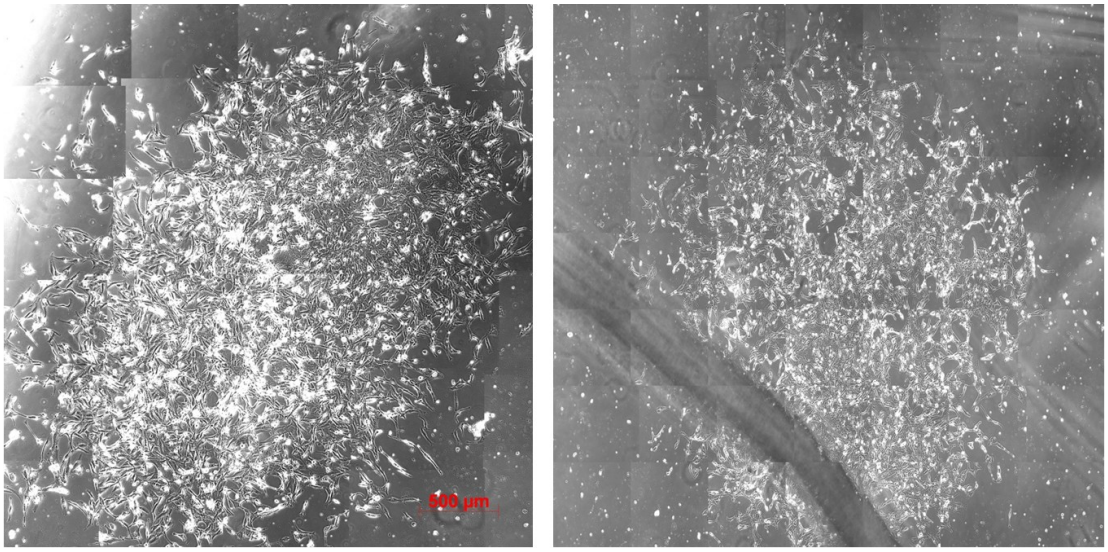


Figure 18. Colonies grew out from control mitochondria dump plates

Identifying colonies from the mitochondria dump control plates is undesirable, since it contradicts with our hypothesis. We hypothesized that control dump plate should have no survivor cells because these rho 0 never received wild-type mitochondria. The fact that some rho 0 stayed alive during the selection indicates that we need to re-consider the uridine-free media selection approach, so that we can have a scheme that only selects out the rho 0 cells being rescued an no longer need uridine to survive.

3.7 Immunofluorescence for LC3 autophagy marker

Previous qualitative confocal imaging proved successful delivery of the respiring DsRedMito HEK293 mitochondria into recipient rho 0 cells. However, the negative result from the qRT-PCR data indicates that for some unknown mechanisms, the delivered mitochondria were not incorporated in the rho 0 network, and no wild-type mtDNA was found. Based on this information, we suspect that delivered mitochondria were eliminated by a process called autophagy in rho 0 cells.

To test for such possibility, we performed immunostaining with autophagy marker LC3. Figure 19 is a LC3 immunofluorescence experiment for a sample 6 hours post mitochondria delivery. Blue indicates LC3 autophagy marker; red represents the DsRedMito HEK293 mitochondria; green is the co-injected FITC-dextran dye to outline cell shape. No overlapping between red and blue was found, suggesting no autophagy in rho 0 cells. This also concludes that autophagy was not the reason that mtDNA failed to incorporate with endogenous mitochondria network. We need to look back to the quality of our isolated mitochondria for more hints.

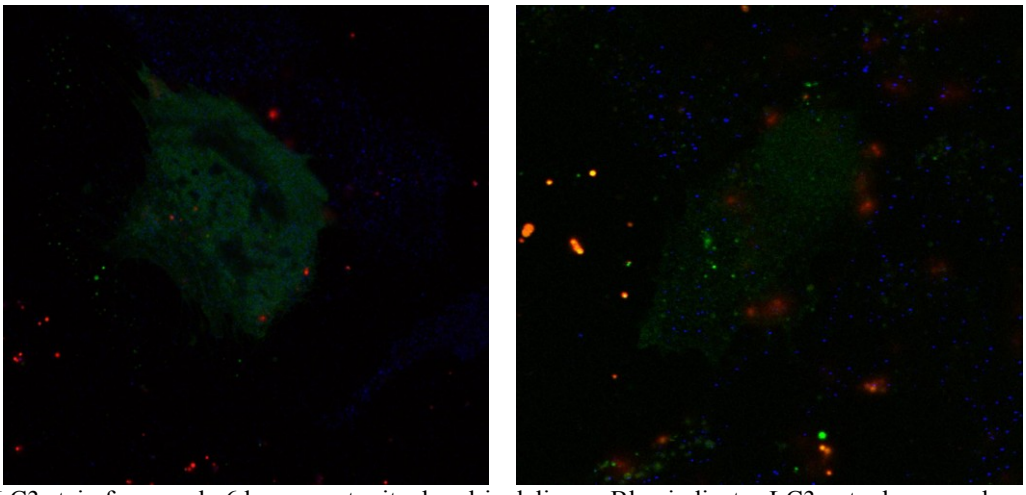


Figure 19. LC3 stain for sample 6 hours post mitochondria delivery. Blue indicates LC3 autophagy marker; red represents the DsRedMito HEK293 mitochondria; green is the co-injected FITC-dextran dye to outline cell shape. No overlapping between red and blue was found, suggesting no autophagy in rho 0 cells.

4. Conclusion

The aim of this project is to improve the respiration defect of mtDNA-depleted osteosarcoma rho 0 cells by photothermal nanoblade delivery of wild-type mitochondria, and to validate the high efficiency of photothermal nanoblade as a novel method of delivering large cellular substances such as mitochondria. We have accomplished several goals while working toward the final target.

We have isolated respiring yet uncoupled wild-type mitochondria from an engineered DsRedMito HEK293 line. We have also shown successful delivery into rho 0 cells with high recipient cell viability, demonstrating the feasibility of photothermal nanoblade as a large cargo delivery tool. However, repeated experiments indicate that uridine-free media selection scheme is not efficiency enough to select a population with improved rho 0 respiration. qRT-PCR data also shows no mtDNA in the recipient rho 0 cells 8 weeks post delivery. A series of mitochondria characterization eliminated the possibility of mitochondrial autophagy,

Clark-type oxygen electrode data shows that we have respiring isolated mitochondria, suggesting complex I-IV of electron transport chain located in the inner membrane is intact and functional. However, the fact that no coupling effect was identified indicates that the outer mitochondrial membrane was ruptured and thus lost the proton gradient. Initially, we concerned weather our isolated mitochondria contain wild-type mtDNA, due to its important role in restoring the rho 0 defected respiration. With our intact mitochondrial inner membrane, the mtDNA can still be maintained in the lumen of isolated mitochondria. Nevertheless, the downstream selection experiments did not result in colonies with improved respiration, suggesting that chemiosmotic coupled isolated mitochondria could be the key to cellular uptake of the delivered mtDNA.

Certainly, there can be other reasons that prevent us from achieving our final purpose of improving defected rho 0 respiration. However, based on the famous study published in *Cell* by King and Attardi in 1988, delivery of mitochondria in to human cells seemed to be able to lead to a rapid replacement of the endogenous mtDNA (King et al. 1988). If the claims in this paper are indeed accurate, we believe that we not only can identify the same mtDNA replacement, but also do it with a higher efficiency using photothermal nanoblade. Our work has achieved several milestones in this project, and more future works will be conducted following the right direction.

References

Ciafaloni E, Ricci E, Shanske S, et al. "MELAS: Clinical features, biochemistry, and molecular genetics." Annals of Neurology. 1992; 31:4, 391-398.

Chandel NS, Schumacker PT. "Cells depleted of mitochondrial DNA (rho0) yield insight into physiological mechanisms." *FEBS Letters.* 1999 Jul 9;454(3):173-6.

French, C.T., Toesca, I.J., Wu, T.-H., Teslaa, T., Beaty, S.M., Wong, W., Liu, M.H., Schroeder, I.S., Chiou, P.-Y., Teitell, M.A., and Miller, J.F. "Dissection of the Burkholderia Intracellular Lifecycle Using a Photothermal Nanoblade." *PNAS*, 2011 July; 108(29): 12095-12100

Gregoire, M., Morais, R., Quilliam, M.A., Gravel, D.," On Auxotrophy for Pyrimidines of Respiration-deficient Chick Embryo Cells." *Eur. J. Biochem*. 1984, 142, 49.

Hatefi, Y., "The mitochondrial electron transport and oxidative phosphorylation system." *Annu Rev Biochem*, 1985; 54:1015-69.

Hayashi JI, Ohta S, Kikuchi A, Takemitsu M, Goto YI, Nonaka I. "Introduction of disease-related mitochondrial DNA deletions into HeLa cells lacking mitochondrial DNA results in mitochondrial dysfunction." *Pro. Natl. Acad. Sci.* 1991; 88:10614-10618.

Hirano M, Pavlakis SG. "Mitochondrial myopathy, encephalopathy, lactic acidosis and stroke-like episodes (MELAS): current concepts." *Journal of Child Neurology*. 1994; 9:4-13.

King, M.P., Attardi, G., "Injection of Mitochondria into Human Cells Leads to a Rapid Replacement of the Endogenous Mitochondrial DNA". *Cell* 1988, v52, 811-819

Lapotko, DO., Lukianova, E., Oraevsky AA. "Selective laser nano-thermolysis of human leukemia cells with microbubbles generated around clusters of gold nanoparticles." *Laser Surg. Med.* 2006 38, 631-642

Li R, Chomyn A, Guan MX. "Human mitochondrial leucyl-tRNA synthetase corrected mitochondrial dysfunctions due to the MELAS and diabetes associated tRNA A3243G mutation." *Mol. Cell. Biol.* 2010.

Ono T., Isobe K., Nakada K., Hayashi J. "Human cells are protected from mitochondrial dysfunction by complementation of DNA products in fused mitochondria". *Nature Genetics* 2001 28, 272-275.

Singh B, Low PS, Yeo JF. "MELAS: A Case Report." *Ann Acad Med Singapore*. 2004; 33:69-71.

Wallace DC. "A Mitochondrial Paradigm of Metabolic and Degenerative Diseases, Aging, and Cancer: A Dawn for Evolutionary Medicine." *Annu. Rev. Genet*. 2005.39:359-407.

Wu TH, TeSlaa T, Teitell MA, Chiou PY. "Photothermal nanoblade for patterned cell membrane cutting." *Optical Society of America*. 2010.

Wu TH, Kalim S, Callahan C, Teitell MA, Chiou PY. "Image patterned molecular delivery into live cells using gold particle coated substrates." *Optical Express*. 2010; 18:938-946.

Yang, J., Liu, X., Bhalla, K., Kim, C.N., Ibrado, A. M., Cai, J., Peng, T., Jones, D. P., Wang, X. "Prevention of Apoptosis by Bcl-2: Release of Cytochrome c from Mitochondria Blocked." *Science* 1997, v275, 1129-1132